SUPPLEMENTARY INFORMATION

Marine biogenic humic substances control iron biogeochemistry across the Southern Ocean

Hassler, C.S.[1,2,3] ; Simó, R.[4]; Fawcett, S.E.[5,6]; Ellwood, M.J.[7,8] ; Jaccard, S.L.[3]

[1] Department F.-A. Forel for environmental and aquatic sciences, University of Geneva, Geneva, Switzerland.

[2] School of Architecture, Civil, and environmental engineering, Smart Environmental Sensing in Extreme Environements, ALPOLE, Ecole Polytechnique Fédérale de Lausanne, Sion, Switzerland.

[3] Institute of Earth Sciences, University of Lausanne, Lausanne, Switzerland.

[4] Institut de Ciències del Mar, ICM-CSIC, Barcelona, Catalonia, Spain.

[5] Department of Oceanography, University of Cape Town, Rondebosch, South Africa.

[6] Marine and Antarctic Research Centre for Innovation and Sustainability, University of Cape Town, Rondebosch, South Africa.

[7] Research School of Earth Sciences, Australian National University, Canberra, Australia.

[8] Australian Centre for Excellence in Antarctic Science (ACEAS), Australian National University, Canberra, Australia.

Supplementary methods

Particulate analyses.

Microbial abundances. Samples (2 to 5 ml each) were fixed with 1% paraformaldehyde plus 0.05% glutaraldehyde (final concentrations) for 15 min at room temperature and stored at -80°C. For enumeration of heterotrophic prokaryotes (mostly bacteria), thawed samples were stained with SYBRgreen I (Molecular Probes; ~20 µM final concentration) prior to quantification by green fluorescence on a flow cytometer (CyFlow Cube 8, Sysmex Partec). Prokaryotic and eukaryotic pico- and nanophytoplankton were also counted on the flow cytometer based on their red and orange autofluorescence[1].

Biogenic silicate (BSi). Seawater samples were collected from the underway seawater supply, filtered on board and then analysed by flow injection following appropriate digestion[2] to yield Bsi concentrations (µM).

Particulate organic carbon (POC). Seawater was filtered through pre-combusted (450°C for 8 hr) glass fibre filters (GF-75s; 0.3 µm pore size; Sterlitech) that were then stored in pre-combusted foil envelopes at -80°C pending analysis. In the laboratory, the POC filters were dried at 40°C for 24 hr, then folded into tin capsules that were analysed for C content using a Flash 2000 elemental analyser coupled to a Delta V Plus isotope ratio mass spectrometer in a configuration with a detection limit of 2 µg C. A range of known masses of three in-house standards were analysed alongside the samples, with the resultant relationship of measured standard peak area to mass used to convert sample peaks areas to C mass. POC concentration was calculated by normalizing C mass to seawater volume filtered[3,4].

Phytoplankton. Pigments and CHEMTAX analyses were done as in [5]. Chemtax and photosynthetic maximum quantum yield (Fv/Fm) were kindly communicated by C. Robinson.

Supplementary Figures and Tables

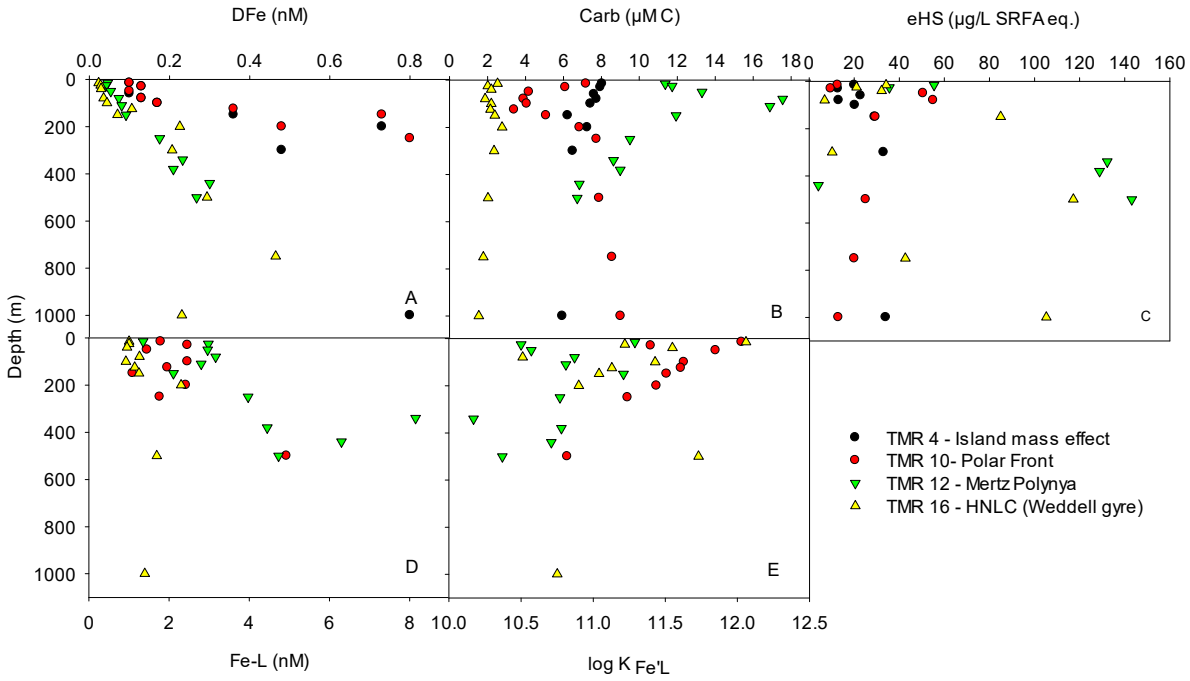

Supplementary Fig. 1. Representation of chemical parameters for contrasted regions of the Southern Ocean. The dissolved Fe (DFe, panel A), hydrolysable carbohydrates (Carb, Panel B), electroactive humic substances (eHS, panel C), Fe-binding ligands (Fe-L, panel D), and the log of the conditional stability constant (log $K_{Fe'L}$, panel E) are shown. These regions include area influenced by island mass effect, Polar Front, polynya and typical High Nutrient Low Chlorophyll (HNLC) region of the Southern Ocean. These stations represent a subset of the station sampled during the ACE expedition.

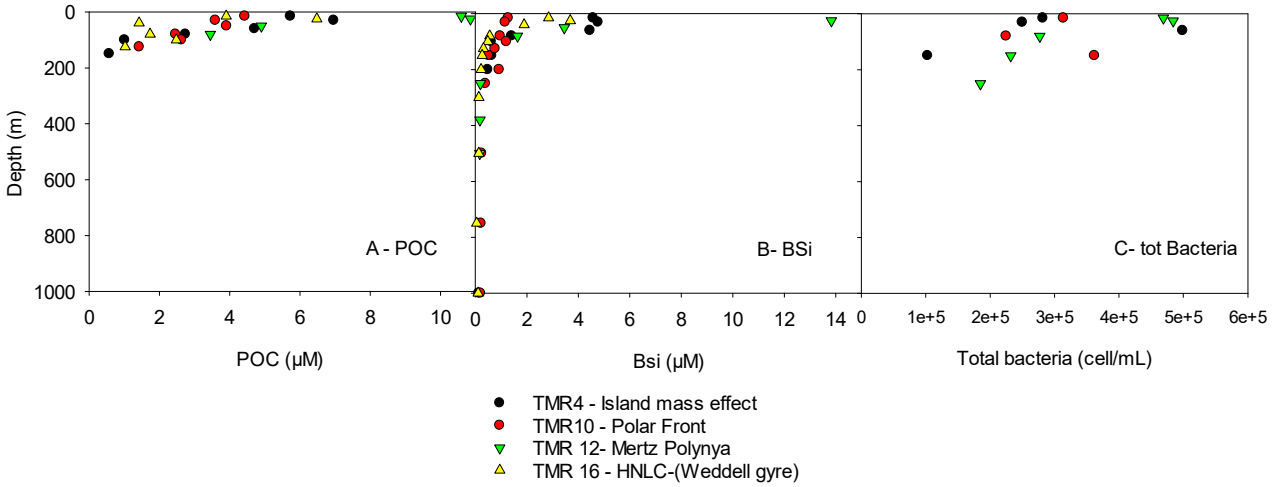

Supplementary Fig. 2. Representation of biological parameters for contrasted regions of the Southern Ocean. The particulate organic carbon (POC, panel A), biogenic silicate (BSi, Panel B), and total heterotrophic bacteria cellular abundance (panel C) are shown. These regions include area influenced by island mass effect, Polar Front, polynya and typical High Nutrient Low Chlorophyll (HNLC) region of the Southern Ocean. These stations represent a subset of the station sampled during the ACE expedition.

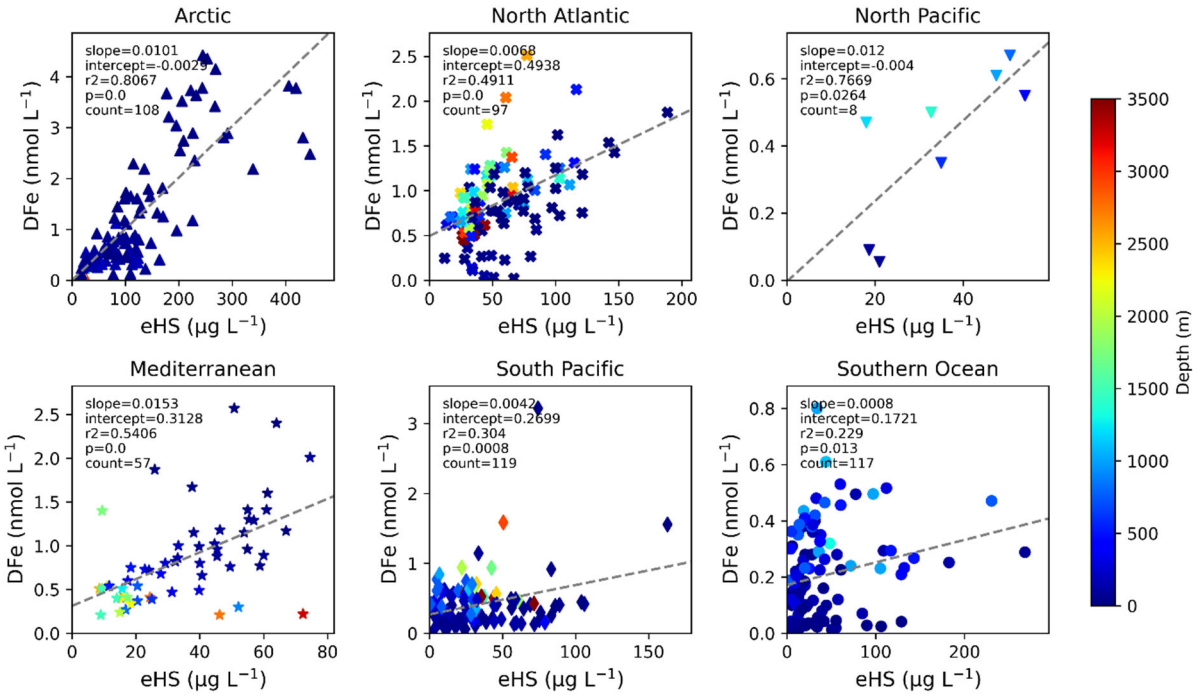

Supplementary Fig. 3. Relationship between DFe, eHS and depth in different ocean basins. Dara are shown for the Arctic[6,7]; North Atlantic[8,9]; North Pacific[8]; Mediterranean Sea[9,10]; South Pacific[11,12]; and Southern Ocean [8](this study). Regression parameters are indicated for each of the ocean basin and sea represented.

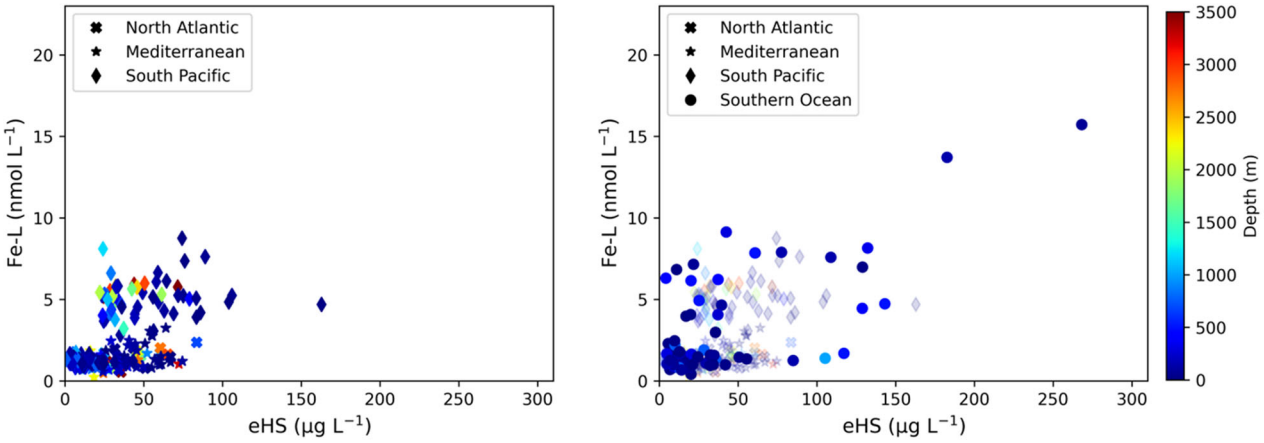

72

73 **Supplementary Fig. 4. Relationship between Fe-L and eHS, and depth in different ocean basins.** Data

74 are shown for the North Atlantic[8,9]; Mediterranean Sea[9,10]; South Pacific[11,12]; and Southern Ocean [8](this

75 study). No Arctic and North Pacific iron-binding ligands were available on the selected studies. All Fe-L

76 data were derived using SA as the exchange ligand, except for the Mediterranean Sea where TAC was

77 used.

78

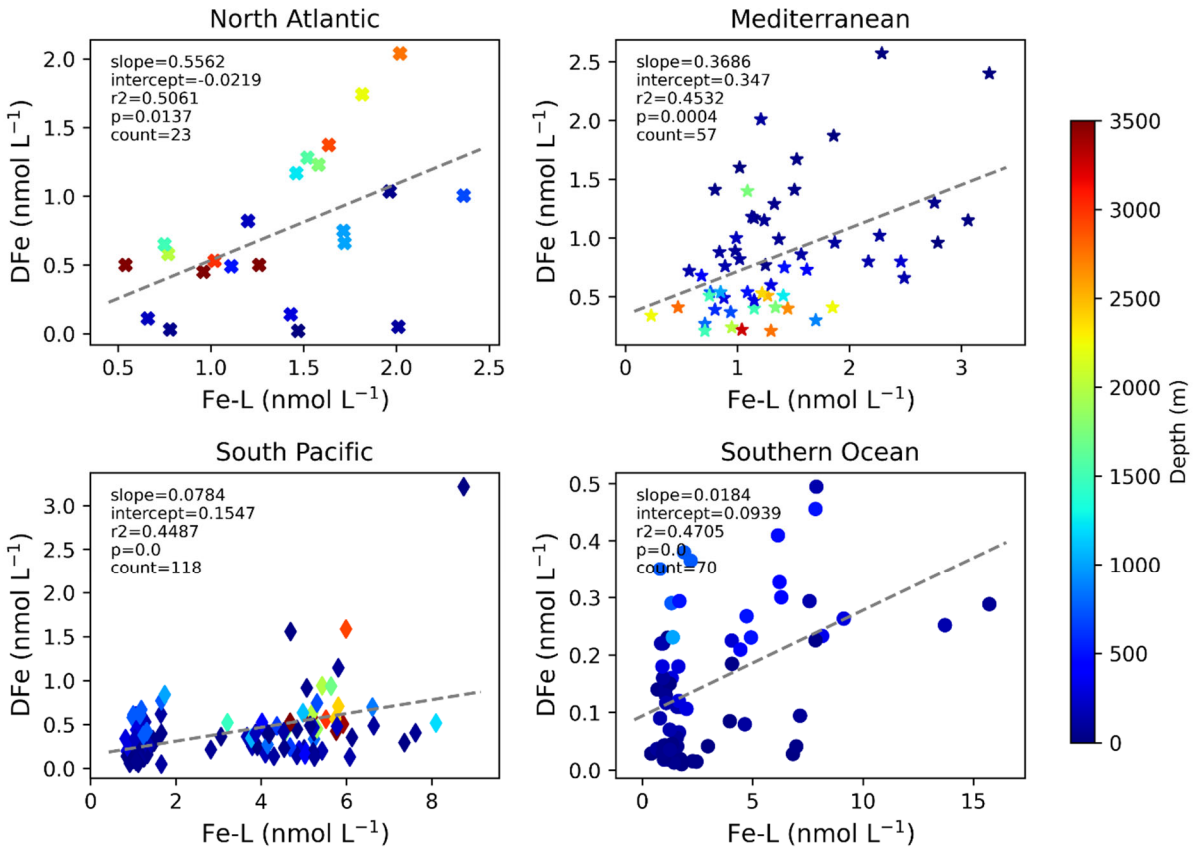

79
80

81 **Supplementary Figure 5. Relationship between DFe and Fe-L in different ocean basins**. Dara are

82 shown for the North Atlantic[8,9]; Mediterranean Sea[9,10]; South Pacific[11,12]; and Southern Ocean [8](this

83 study). No Arctic and North Pacific iron-binding ligands were available on the selected studies.

84 Regression parameters are indicated for each of the ocean basin and sea represented.

85

Supplementary Table 1. Antarctic Circumnavigation Expedition (ACE) stations – Cape Town to Hobart (Leg 1, 20-December-2016 to 19-January-2017, TMR stations 3–7) and Hobart to Punta Arenas (Leg 2, 22-January-2017 to 22-February-2017, TMR stations 8–20) – onboard the R/V Akademik Tryoshnikov.

Stn #	TMR #	Date	Lat	Long
16	3	07.01.2017	-50.994	72.04
19	4	09.01.2017	-53.133	81.721
20	5	11.01.2017	-54.825	95.684
21	6	14.01.2017	-53.198	118.134
22	7	17.01.2017	-46.906	141.931
23	8	23.01.2017	-46.393	150.3888
24	9	25.01.2017	-53.5825	149.2976
25	10	26.01.2017	-59.6105	148.6399
26	11	29.01.2017	-67.1036	144.9204
36	12	30.01.2017	-67.1895	145.7209
43	13	31.01.2017	-65.9932	159.0105
47	14	04.02.2017	-67.2897	163.536
49	15	05.02.2017	-67.0999	167.3602
56	16	09.02.2017	-71.6993	-143.6983
68	17	14.02.2017	-68.7486	-99.9592
71	18	18.02.2017	-63.9631	-66.2425
72	19	18.02.2017	-62.5089	-68.0376
73	20	19.02.2017	-59.5999	-67.9187

Supplementary Table 2. Pearson correlations table between selected parameters considering data for the full water column (0-1000m). Selected parameters are depth, dissolved Fe (DFe), Fe-binding ligands (Fe-L) with their conditional stability constant (log $K_{Fe'L}$), hydrolysable carbohydrates (Carb), electroactive humic substances (eHS) and total bacterial cell abundance (Bacttot). Statistically significant ($p < 0.05$) positive and negative correlations are highlighted in green and red, respectively. Data show coefficient of correlation (R) on top, p value (p) and number of observations at the bottom.

	DFe	Fe-L	log K	Carb	eHS	Bacttot
depth	0.623	0.0634	-0.0124	-0.213	0.163	-0.262
	5.45E-27	0.491	0.893	0.000942	0.0944	0.0155
	238	120	120	239	106	85
DFe		0.487	-0.0874	-0.296	0.245	-0.291
		1.65E-08	0.342	0.00000352	0.0119	0.00721
		120	120	237	105	84
Fe-L			-0.22	0.0897	**0.699**	**-0.416**
			0.0156	0.33	**1.76E-11**	**0.00451**
			120	120	**70**	**45**
log K				-0.0807	-0.262	-0.13
				0.381	0.0287	0.393
				120	70	45
Carb					-0.0547	**0.395**
					0.578	**0.000185**
					106	**85**
eHS						**-0.397**
						0.00637
						46

Supplementary Table 3. Pearson correlations table between selected parameters considering data for the surface water only (0-100m). Selected parameters are dissolved Fe (DFe), Fe-binding ligands (Fe-L) with their conditional stability constant (log $K_{Fe'L}$), hydrolysable carbohydrates (Carb), electroactive humic substances (eHS), particulate organic carbon (POC) biogenic silicate (BSi), and maximum effective quantum yield (Fv/Fm). Flow cytometry derived cellular abundances is shown for total bacteria (totBact), Synechococcus (Syn), Picoeukarotes (Picoeuk 1 and 2), Nanoeukaryotes (Nanoeuk) and Cryptomonas. Phytoplankton classes derived from pigments and CHEMTAX analysis are also shown for Chlorophytes (Chloro), Cryptophytes (Crypto), Cyanobacteria (Cyano), Diatoms (Diat A and B), Dinophytes (Dino), Haptophytes (Hapto8 and 67), Prasinophytes (Pras) and Pelagophytes (Pelago). Statistically significant ($p < 0.05$) positive and negative correlations are highlighted in green and red, respectively. Data show coefficient of correlation (R) on top, p value (p) and number of observations at the bottom.

	Fe-L	log K	Carb	eHS	Bsi	POC	Bacttot	Syn	Picoeuk1	Picoeuk2	Nanoeuk	Cryoptomon	Chloro	Crypto	Cyano	DiatA	DiatB	Dino	Hapto8	Hapto67	Pras	Pelago	Fv/Fm
DFe	0.462	-0.251	-0.000496	0.11	-0.123	-0.0276	-0.113	-0.0844	-0.0644	-0.288	0.0235	-0.278	-0.128	0.0322	-0.237	0.00466	-0.0894	-0.17	0.214	-0.0194	-0.0784	-0.165	0.164
	0.000437	0.0673	0.996	0.419	0.234	0.79	0.377	0.518	0.616	0.022	0.855	0.0287	0.223	0.761	0.0231	0.965	0.397	0.106	0.0407	0.855	0.458	0.115	0.121
	54	54	101	56	96	96	63	61	63	63	63	62	92	92	92	92	92	92	92	92	92	92	90
Fe-L		-0.113	0.197	**0.801**	-0.118	-0.31	-0.2	-0.299	-0.0853	0.154	0.0132	0.153	-0.135	0.125	-0.221	-0.132	-0.0885	-0.365	0.0406	-0.233	-0.00533	-0.232	**0.518**
		0.417	0.154	**9.18E-10**	0.413	0.027	0.274	0.103	0.643	0.4	0.943	0.41	0.366	0.402	0.135	0.378	0.554	0.0117	0.786	0.115	0.972	0.117	**0.000268**
		54	54	**39**	50	51	32	31	32	32	32	31	47	47	47	47	47	47	47	47	47	47	**45**
log K			-0.112	-0.111	-0.239	-0.231	-0.323	-0.0645	0.0243	-0.151	-0.359	0.0899	-0.147	-0.252	-0.0744	-0.0661	-0.229	0.0816	0.0012	-0.18	-0.0667	-0.11	0.0798
			0.421	0.501	0.0946	0.103	0.0712	0.73	0.895	0.408	0.0437	0.631	0.323	0.0876	0.619	0.659	0.122	0.585	0.994	0.227	0.656	0.461	0.602
			54	39	50	51	32	31	32	32	32	31	47	47	47	47	47	47	47	47	47	47	45
Carb				-0.0297	0.0268	0.101	0.432	0.485	0.47	0.435	0.337	0.254	0.454	-0.0382	0.293	0.07	0.114	0.399	0.19	0.515	0.204	0.314	0.141
				0.828	0.794	0.324	0.000368	0.0000649	0.0000904	0.000333	0.00654	0.045	0.00000479	0.716	0.00444	0.505	0.275	0.000075	0.0687	0.00000013	0.0494	0.00216	0.183
				56	97	97	64	62	64	64	64	63	93	93	93	93	93	93	93	93	93	93	91
eHS					-0.0462	-0.174	-0.161	-0.224	-0.336	-0.218	-0.0744	-0.0391	-0.209	-0.0386	-0.186	-0.0585	0.0267	-0.188	-0.099	-0.252	-0.0792	-0.266	**0.307**
					0.748	0.212	0.38	0.226	0.0602	0.23	0.686	0.835	0.149	0.792	0.201	0.69	0.855	0.195	0.499	0.0802	0.588	0.0647	**0.036**
					51	53	32	31	32	32	32	31	49	49	49	49	49	49	49	49	49	49	**47**

Supplementary References

1 Simó, R., Zamanillo, M., and Castillo, Y. Bacterial and phytoplankton abundances by flow cytometry - collected from the Southern Ocean in the austral summer of 2016/2017, during the Antarctic Circumnavigation Expedition. *Zenodo,* https://zenodo.org/records/11520826 (2024).

2 Hassler, C. & Ellwood, M. Biogenic silicate concentration in seawater samples, collected from the CTD in the Southern Ocean during the austral summer of 2016/2016, on board the Antarctic Circumnavigation Expedition. *Zenodo* https://doi:10.5281/zenodo.2621103 (2019).

3 Stirnimann, L. & Fawcett, S.E. Isotope ratios, carbon and nitrogen concentrations, and phytoplankton composition data from the ACE Expedition [Data set] *Zenodo* https://doi.org/10.5281/zenodo.8422942 (2023)

4 Stirnimann, L., Bornmann, T., Forrer, H.J., et al. A circum-Antarctic plankton isoscape: carbon export potential across the summertime Southern Ocean. *Global Biogeochemical Cycles* 38, e2023GB007808, https://doi.org/10.1029/2023GB007808 (2023).

5 Antoine, D. et al. Phytoplankton pigment concentrations of seawater sampled during the Antarctic Circumnavigation Expedition (ACE) duiring the austral summer of 2016/2017. *Zenodo* https://doi: 10.5281/zenodo.3816726 (2019).

6 Slagter, H.A., Laglera, L.M., Sukekava, C. & Gerringa, L.J.A. Fe-binding organic ligands in the humic-rich TransPolar Drift in the surface Arctic Ocean using multiple voltammetric methods. Journal of Geophysical Research **124**,1491-1508 (2019).

7 Laglera, L.M. et al. First quantification of the controlling role of humic substances in the transport of iron across the surface of the Arctic Ocean. Environmental Science & Technology **53**, 13136-13145 (2019).

8 Whitby, H. et al. A call for refining the role of humic-like substances in the oceanic iron cycle. *Sci. Rep.* https://doi.org/10.1038/s41598-020-62266-7 (2020).

9 Dulaquais, G. et al. The biogeochemistry of electroactive humic substances and its connection to iron chemistry in the North East Atlantic and the Western Mediterranean Sea. Journal of Geophysical Research **123**,5481-5499 (2018).

10 Gerringa, L. J. A., Slagter, H. A., Bown, J., van Haren, H., Laan, P., et al. Dissolved Fe and Fe-binding organic ligands in the Mediterranean Sea–GEOTRACES G04. Mar. Chem. **194**, 100–113 (2017).

11 Cabanes, D.J.E. et al. Using Fe chemistry to predict its bioavailability for natural plankton assemblages from the Southern Ocean. *Mar. Chem.* https://doi: 10.1016/j.marchem.2020.103853 (2020).

12 Mahieu, L. et al. Iron-binding by dissolved organic matter in the Western Tropical South Pacific Ocean (GEOTRACES TONGA cruise GPpr14). Frontiers in Marine Science **11**, 304118 (2024).